# Characterisation of Fatigue Damage of Asphaltic Materials

H. Khalid & I. Artamendi
*Department of Civil Engineering, University of Liverpool, Liverpool, UK*

ABSTRACT: Four-point bending fatigue tests were conducted on asphalt specimens under controlled strain and stress to study damage evolution using the stiffness modulus. A common feature in these tests, irrespective of mode, was that modulus deterioration could be split into three phases; initial (rapid deterioration), intermediate and final in which failure occurred. Damage was modelled based on behaviour at the intermediate phase during which the modulus appeared to follow a straight-line v number of cycles. The effect of test mode on fatigue behaviour was facilitated by the inclusion in the model of a dissipated energy parameter, measured over the intermediate modulus evolution phase. A simple iterative approach was adopted in the model to produce a unique damage parameter that describes the material's fatigue performance independent of test mode. The damage concept was applied to two asphalt mixtures; a stone mastic asphalt (SMA) used as surfacing on major roads and a dense bitumen macadam (DBM) used as binder course on lightly trafficked roads. The effect of binder modification on resistance to fatigue damage was also included in the study. The SMA binder was modified by the addition of different quantities of crumb rubber modifier (CRM) obtained from truck tyres to study the effect of CRM content. The DBM binder was modified by the addition of CRM from truck and car-tyres to study the effect of CRM origin. When plotted v initial strain, the deduced damage parameter showed a clear distinction in ranking the mixtures in accordance with their fatigue performance.

KEY WORDS: Fatigue cracking, damage depiction, rubber-modified asphalt

## 1 INTRODUCTION

Load-induced fatigue cracking is a serious distress mode that could lead to significant damage and consequent failure of flexible pavements. Asphalt fatigue performance can be predicted from cyclic bending laboratory tests, which enable the accurate assessment of damage measured in terms of the gradual deterioration of the material's stiffness modulus. Classical bending fatigue tests are conducted under either controlled strain or stress mode, although damage itself is a structural condition that occurs after a certain number of load applications irrespective of test mode. The aim of this paper is to arrive at a damage model combining the two fatigue modes into a unique equation representative of a specific material. To achieve this aim, four-point bending fatigue tests were conducted on two conventional asphalt mixtures of different design and service requirements, namely a macadam and a stone mastic asphalt. These mixtures were also modified by adding crumb rubber from waste tyres using the wet process technology to study the effect of rubber modification on fatigue behaviour.

## 2 MATERIALS

In this study, two penetration-grade binders were employed, a 50 and 100 Pen, from two different sources, namely Middle Eastern from Kuwait (KSR) and Venezuelan (VEN) respectively. The 50 Pen KSR bitumen was modified by adding 5 and 10 % Crumb Rubber Modifier (CRM), from truck tyres, by weight of binder. The 100 Pen VEN, on the other hand, was modified by adding 10 % CRM, from truck and from car tyres, by weight of binder. The CRM from waste vehicle tyres used to modify the two binders was produced by ambient shredding followed by mechanical grinding to specific sizes. CRM mesh sizes of 30 and 50, i.e. 600 and 300μm nominal maximum particle size, were used to modify the 100 and 50 Pen binders respectively.

CRM modified binders were produced using a high-shear mixer under controlled conditions of temperature, duration and shear rate. Specific quantities of CRM were added to the hot bitumen at 180 $^0$C and mixed for 1 hour at 2000 rpm in 1-litre flasks placed on an iso-mantle heater and covered with an insulation mantle. During the mixing process, the temperature of the rubber-bitumen blend was monitored.

The 50 Pen KSR binder was used in the design of a stone mastic asphalt (SMA) suitable for surface courses of heavily trafficked roads, such us motorways, whereas the 100 Pen VEN binder was used in the design of a dense bitumen macadam (DBM) used on lightly trafficked roads. The principle adopted in mixture design was the volumetric control of the internal void structure of the asphalt mixture. Gritstone aggregates, 14 mm maximum nominal size, and limestone filler (<75 μm) were used in both mixtures.

The control SMA mixture was designed at a binder content of 5.5 %, which resulted in 5.1 % void content. Customary SMA application practice involves inclusion of cellulose fibres and these were included at 0.3 % of binder. With respect to CRM modification, at 5 % CRM, the design binder content was the same as that of the control mixture, i.e. 5.5 % of total mixture. However, at 10 % CRM, the binder content had to be increased to compensate for the reduced amount of bitumen in the binder and to restore the mobility of the binder, which is slowed down due to the absorption of its mobile components by the rubber. Thus, 6.0 % binder content was used, which resulted in 4.0 % void content. Fibres were not incorporated into the modified SMA mixtures. Similarly, the control DBM mixture was designed at a binder content of 4.8 %, which resulted in 5.6 % void content, whereas the two modified DBM mixtures were designed at binder content of 5.8 %, giving 3.5 % void content. Details of the mixtures used in the study are presented in Table 1.

Table 1:Details of the mixtures used in the study

| Mixture | Bitumen | | CRM | | | Binder content (%) | Void content (%) |
|---|---|---|---|---|---|---|---|
| | Grade | Origin | Content (%) | Size (μm) | Source | | |
| DBM Control | 100 Pen | VEN | 0 | | | 4.8 | 5.6 |
| DBM 1 | | | 10 | 600 | Truck-tyre | 5.8 | 3.5 |
| DBM 2 | | | 10 | 600 | Car-tyre | 5.8 | 3.5 |
| SMA Control | 50 Pen | KSR | 0 | | | 5.5 | 5.1 |
| SMA 1 | | | 5 | 300 | Truck-tyre | 5.5 | 5.2 |
| SMA 2 | | | 10 | 300 | Truck-tyre | 6 | 4.0 |

## 3 LABORATORY FATIGUE TESTS

Fatigue testing was performed in a four-point bending (4PB) test apparatus under controlled strain (deflection) and stress (load) conditions. The test set-up consisted of a servo-hydraulic testing system equipped with a 2.5 kN load cell mounted above the fatigue frame. The asphalt specimen was clamped in position at the four points of the fatigue frame by means of torque motors located underneath the four supports. The vertical deflection at the centre of the beam was measured using a linear variable differential transducer (LVDT) situated at the bottom of the beam. The vertical deflection and the applied load were used to determine the magnitude of the strains and stresses during each load cycle. Furthermore, phase lag between stress and strain and dissipated energy, i.e. the area within the hysteresis loop, were also computed during the tests.

The asphalt mixtures were compacted to slabs using a laboratory rolling wheel compactor. Beam specimens of 300x50x50 $mm^3$ were cut from the slabs and used for fatigue testing. During fatigue tests, the specimens were subjected to sinusoidal oscillating axial loading in both tension and compression at a frequency of 10 Hz with no rest periods. All tests were conducted at a temperature of 10 $^0$C. Fatigue tests finished when the stiffness modulus reached 50 % of the initial value for both controlled strain and stress test modes. For controlled strain tests, strain amplitudes selected varied between 125 and 215 μm/mm, whereas for controlled stress tests, stress amplitudes selected varied between 1000 and 2000 kPa. Up to 18 beams were tested for each mixture, about half of them under controlled strain and the other half under controlled stress.

## 4 FATIGUE FAILURE

Traditionally, failure in controlled strain mode has been arbitrarily defined as the number of cycles, $N_f$, to 50 % reduction in the initial stiffness modulus whereas a reduction to 10 % has been used for controlled stress mode. The classical failure criterion, however, has led to inconsistent fatigue results that are, consequently, of limited value. Some limitations of this approach include large scatter among test results, differences between controlled strain and stress tests and dependence of failure on initial stiffness and test temperature (Lundstrom et al., 2003).

Alternatively, Hopman et al. (1989) proposed the use of an energy ratio to define crack initiation as the number of cycles, $N_1$, in a controlled strain fatigue test to a point where cracks are considered to initiate, it is also defined as the coalescence of micro-cracks to form a sharp crack (macro-crack), which then propagates. The $N_1$ failure criterion, therefore, permits a comparison of materials at the same states of damage, corresponding to macro-crack initiation, and avoids arbitrary definition of failure.

In this study, an Energy Ratio, $R_n$, defined as the quotient between the cumulative dissipated energy up to the n-cycle and the dissipated energy at the n-cycle has been used to determine $N_1$ for both test modes. For controlled strain tests, when $R_n$ is plotted against number of cycles there is a change in behaviour at $N_1$, represented by the change of the slope at this point. For controlled stress test, on the other hand, $N_1$ is determined from the peak value of $R_n$. The accurate determination of $N_1$ is, however, more difficult for controlled strain tests compared to controlled stress tests (Rowe, 1993).

Fatigue results for controlled strain and stress tests have been used to derive a relationship between the initial strain, $\varepsilon_0$, and stress, $\sigma_0$, and fatigue failure, $N_1$, as follows:

$$N_1 = C_1\left(\frac{1}{e_0}\right)^m \quad \text{and} \quad N_1 = C_2\left(\frac{1}{s_0}\right)^n \tag{1}$$

where $C_1$, m, $C_2$ and n are material constants. The initial values of the strains and stresses were defined as the values at 100 load cycles calculated by linear regression of the first 500 cycles, as some variability was observed during the first few cycles. Figure 1 shows typical fatigue test results expressed as linear relationships between tensile strain or stress, and number of cycles to failure, when plotted using logarithmic scales. Materials regression constants are presented in Table 2.

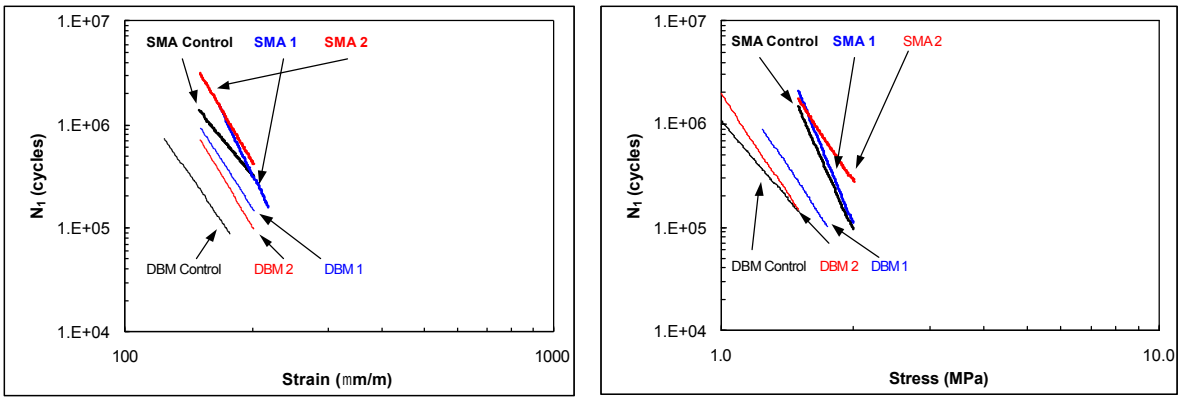


Figure 1: Controlled strain and stress fatigue test results

Longer fatigue lives for the SMA mixture were attributed to volumetric composition and bitumen grade. Also, CRM modification enhanced the fatigue behaviour of the two mixtures. For the DBM, the mixture modified with truck-tyre rubber (DBM 1) gives longer fatigue lives than that with car-tyre rubber (DBM 2). For the SMA, the fatigue behaviour improves with increased CRM content, i.e. at 5% CRM (SMA 1) the fatigue life was shorter than at 10 % CRM (SMA 2). For instance, for controlled strain tests the tensile strain at $10^6$ load cycles, $\varepsilon_6$, gives an indication of the improved fatigue performance of the rubber-modified mixtures, as shown in Table 2.

Table 2: Regression coefficients and materials constants

| Mixture | Controlled strain mode | | | | Controlled stress mode | | |
|---|---|---|---|---|---|---|---|
| | $C_1$ | m | $R^2$ | $\varepsilon_6$ (μm/m) | $C_2$ | n | $R^2$ |
| DBM Control | 2.0E+18 | 5.97 | 0.91 | 114.9 | 1.0E+06 | 4.99 | 0.76 |
| DBM 1 | 6.0E+19 | 6.33 | 0.89 | 150.2 | 4.0E+06 | 6.40 | 0.89 |
| DBM 2 | 4.0E+20 | 6.79 | 0.75 | 141.4 | 2.0E+06 | 6.34 | 0.97 |
| SMA Control | 9.0E+16 | 4.97 | 0.81 | 160.0 | 7.0E+07 | 9.44 | 0.91 |
| SMA 1 | 2.0E+25 | 8.60 | 0.76 | 175.5 | 1.0E+08 | 10.19 | 0.96 |
| SMA 2 | 3.0E+21 | 6.86 | 0.89 | 180.4 | 2.0E+07 | 6.62 | 0.77 |

## 5 DAMAGE EVOLUTION

### 5.1 Definition of damage

Fatigue data has been generally analysed by plotting the reduction in stiffness against the number of load cycles using logarithmic scales and fitting an exponential relationship to the data (Tayebali et al., 1992). There is, however, no experimental evidence or theoretical basis for a power-law relationship (Rowe and Bouldin, 2000). Di Benedetto et al. (1996), on the other hand, analysed fatigue data from uniaxial tests using linear scales and identified the existence of three phases during a fatigue test; initial, intermediate and final in which failure occurred.

In this study, fatigue results from 4PB tests have also shown the existence of three ph ases, as seen in Figure 3. The first phase, phase I, is characterised by a rapid reduction in stiffness modulus with number of load applications. This rapid decrease in stiffness has been attributed to internal heating of the specimen due to dissipated energy after each load cycle (Di Benedetto et al., 1996), bitumen thixotropy (Neifar and Di Benedetto, 2002) and low adhesion between stone and bitumen resulting in the development of micro-cracks within the bitumen, commencing at aggregate particle contacts (Thom et al., 2002). In phase II, the temperature stabilizes. This phase is characterised by an approximately linear reduction in the stiffness modulus with number of cycles, after the initial rapid decrease in modulus during phase I. Furthermore, Di Benedetto at al. (1996) reported that a fatigue damage law could be isolated and characterized only during phase II. Finally, phase III is characterised by a rapid drop in stiffness modulus with load cycles up to failure. This rapid degradation can be attributed to coalescence of micro-cracks to for a sharp crack (macro-crack).

For the purpose of this paper, phase II has been defined as follows. A straight line was fitted to the stiffness modulus test data for the interval between 30 and 60 % of the number of cycles to 50 % reduction in initial stiffness modulus. It was observed that this interval was always well within the linear region. The limits of phase II were then defined as the interval within which the difference between the experimental and fitted values was less than 1 %.

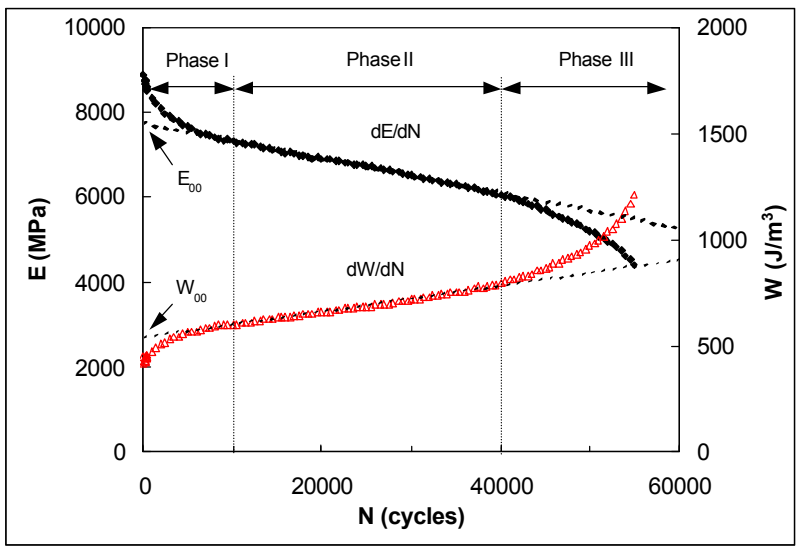


Figure 2: Fatigue phases

Based on the linear reduction in the stiffness modulus in phase II a damage parameter, D, can be introduced. Thus,

$$D(N) = \frac{E_{00} - E(N)}{E_{00}} \tag{2}$$

The damage parameter, D, ranges from 0 (undamaged) to 1 (fully damaged). The rate of damage can be calculated by differentiating Equation 2, as follows,

$$\frac{dD}{dN} = -\frac{1}{E_{00}}\frac{dE}{dN} = -a_T \tag{3}$$

To obtain the rate of damage, dD/dN, a straight line was fitted to the stiffness modulus data in phase II. The point where the extrapolated fitted line intercepted the stiffness modulus axis corresponded to $E_{00}$ and the slope of this line was dE/dN, as shown in Figure 2.

For controlled strain and stress test results, the change in the damage parameter with number of load applications, or rate of damage, obtained using equation 3, was plotted on log-log scales as a function of the initial strain and stress respectively. It was found that data could be fitted by a straight line, indicating a power law relationship between these parameters (Choi et al., 2002), as seen in Figure 3.

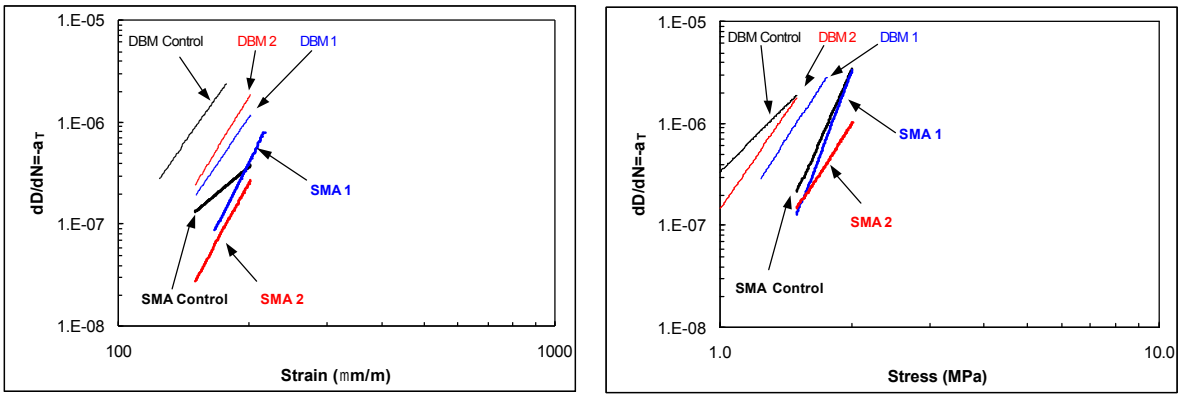


Figure 3: Relationship between the rate of damage and the initial strain and stress

## 5.2 Effect of dissipated energy on rate of damage

The rates of damage for controlled stress tests have also been plotted as a function of the initial strain, defined as before, as seen in Figure 4 for the DBM and SMA control mixtures. It can be observed that, for the same initial strain, the rate of damage for controlled stress tests is higher than that for controlled strain tests, as expected. Differences between the rate of damage for controlled strain and stress tests might be attributed to dissipated energy effects occurring in both test modes. Furthermore, for the same initial strain, differences between damage rates for controlled strain and stress modes for the DMB were much smaller than those for the SMA. This indicates that the SMA is less susceptible to dissipated energy effects occurring during controlled strain and stress test modes.

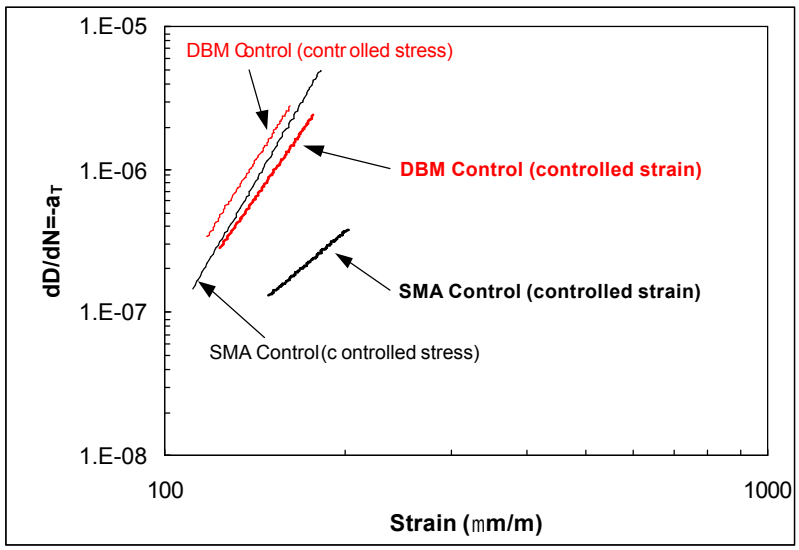


Figure 4: Relationship between rate of damage and initial strain for controlled strain and stress tests

To compare the rate of damage for controlled strain and stress tests, the influence of the thermal effects occurring during phase II must be considered. It has been observed that during controlled strain fatigue testing the dissipated energy decreases with number of load cycles and increases during controlled stress tests. Di Benedetto et al. (1996, 1997 and 2003) assumed that the change in stiffness modulus due to non-fatigue damage effects, primarily thermal and thixotropy effects, is proportional to the dissipated energy. Therefore, the proposed relationship to determine the rate of damage due only to fatigue can be written as follows,

$$\frac{dD^*}{dN} = -a_F = -a_T - C\left(\frac{E_0 - E_{00}}{E_{00}}\right)a_W \tag{4}$$

where $E_0$ is the initial stiffness modulus, i.e. the stiffness at 100 cycles calculated by linear regression of the first 500 cycles; C is a material constant and,

$$a_W = \frac{1}{W_{00}}\frac{dW}{dN} \tag{5}$$

where $W_{00}$ and dW/dN are determined by fitting a straight line to the dissipated energy data in phase II. The point where the extrapolated fitted line intercepted the dissipated energy axis corresponded to $W_{00}$ and the slope of this line is dW/dN, as shown in Figure 2.

It can be seen from Equation 4 that the effect of the dissipated energy term is to reduce the absolute rate of fatigue damage for controlled stress loading, where the dissipated energy increases with load cycles ($a_W>0$), and to increase it for controlled strain loading, where the dissipated energy decreases with load cycles ($a_W<0$). To observe the effect of the energy dissipation parameter on the overall damage evolution model, absolute values of $a_W$ obtained using Equation 5 were plotted on a log-log scale as a function of the initial strain, and a power law relationship between these parameters was found for the DBM and SMA control mixtures, as seen in Figure 5.

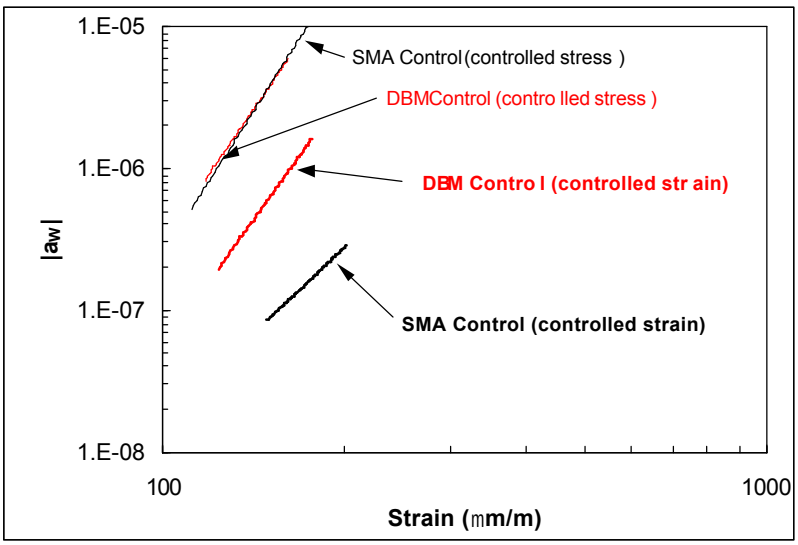


Figure 5: Relationship between rate of energy dissipation and initial strain

If fatigue characterization were an intrinsic property of a material, thus, independent of loading mode, the rate of fatigue damage at a particular strain level should be the same in controlled strain or stress mode. Based on this concept, a power law relationship was found between the rate of fatigue damage, $dD^*/dN$, calculated using Equation 4, and the initial strain for both test modes, as follows,

$$\frac{dD^*}{dN} = A\left(\frac{1}{\varepsilon_0}\right)^B \tag{6}$$

where A and B are materials' constants.

The only remaining unknown parameter in Equation 4 is the constant C. To determine its magnitude for a unique definition of $a_F$, an initial value of zero is assumed, i.e. only $a_T$ contributing to the overall damage. This is followed by a simple iterative incremental process, which aims at maximising the $R^2$ value for the relationship in Equation 4 from the two sets of data, i.e. strain and stress. Materials' constants, $R^2$ and C values for the mixtures investigated are presented in Table 3. The relationship between the rate of fatigue damage, $dD^*/dN$, and initial strain from controlled strain and stress tests for the materials investigated is presented in Figure 6. The figure shows a unique fatigue damage relationship for each material, irrespective of test mode.

Table 3: Materials constants and regression coefficients for the mixtures investigated

| Mixture | $dD^*/dN=A(1/\varepsilon_0)^B$ | | | |
|---|---|---|---|---|
| | A | B | $R^2$ | C |
| DBM Control | 5.0E-19 | 5.66 | 0.81 | 1.95 |
| DBM 1 | 1.0E-15 | 3.91 | 0.75 | 2.70 |
| DBM 2 | 7.0E-17 | 4.53 | 0.84 | 3.05 |
| SMA Control | 9.0E-17 | 4.32 | 0.49 | 2.07 |
| SMA 1 | 2.0E-15 | 3.73 | 0.49 | 1.94 |
| SMA 2 | 4.0E-18 | 4.82 | 0.47 | 1.95 |

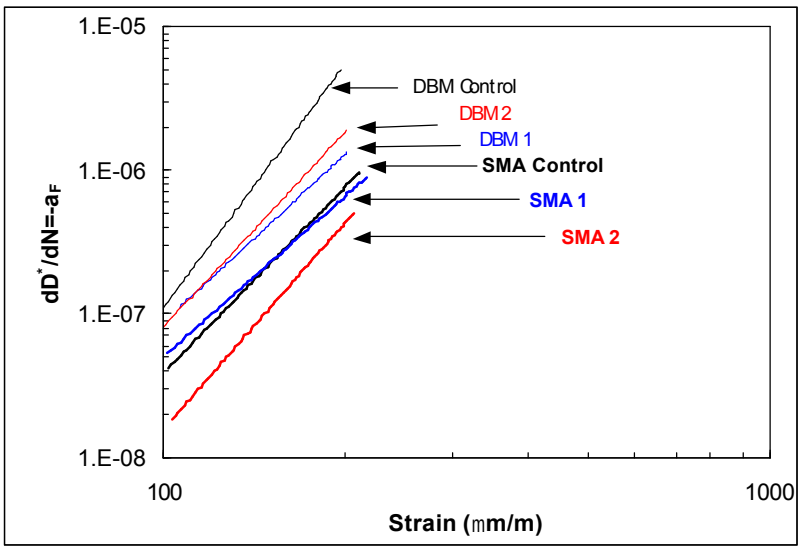


Figure 6: Relationship between the rate of fatigue damage and initial strain from controlled strain and stress tests

## 6 CONCLUSSIONS

A damage model has been developed, which combines fatigue data from controlled strain and stress mode tests. Independent of test mode, the SMA mixture had superior fatigue properties to those of the DBM mixture. Whilst the hypothesis used in deriving the damage model seemed to apply in principle to both mixtures, the distinct difference in fatigue performance of the SMA in controlled strain and stress has led to relatively low correlation coefficients.

It has been shown that the addition of crumb rubber from tyre waste improves asphalt fatigue performance. Crumb rubber from truck tyres has led to better fatigue performance than that from car tyres.

## REFERENCES

Choi, Y. K., Collop, A. C. and Thom, N. H., 2002. *A simple damage approach to modelling fatigue in bituminous materials*. Bearing Capacity of Roads and Airfields, Proceedings of the 6th International Conference, Lisbon, pp. 103-111.

Di Benedetto, H., Ashayer Soltani, M.A. and Chaverot, P., 1996. *Fatigue damage for bituminous mixtures: a pertinent approach*. Proceedings of the Association of Asphalt Paving Technologists, Vol. 65, pp. 142-158.

Di Benedetto, H., Ashayer Soltani, A. and Chaverot, P., 1997. *Fatigue damage for bituminous mixtures*. Mechanical Tests for Bituminous Materials, Proceedings of the 5th International RILEM Symposium, Lyon, pp. 263-270.

Di Benedetto, H., de La Roche, C., Baaj, H., Pronk, A. and Lundstron, R., 2003. *Fatigue of bituminous mixtures: different approaches and RILEM group contribution*. Performance Testing and Evaluation of Bituminous Materials, Proceedings of the 6th International RILEM Symposium, Zurich, pp. 15-38.

Hopman, P.C., Kunst, P.A. and Pronk, A.C., 1989. *A renew interpretation method for fatigue measurements, verification of Miner's Rule*. 4th Eurobitume Symposium, Madrid, pp. 557–561.

Lundstrom, R., Isacsson, U. and Ekblad, J., 2003. *Investigations of stiffness and fatigue properties of asphalt mixtures*. Journal of Materials Science, Vol. 38, pp. 4941-4949.

Neifar, M. and Di Benedetto, H., 2002. *Complex modulus of bituminous mixes: how to interpret measurements*. Proceedings of the 3rd International Conference Bituminous Mixtures and Pavements, Thessaloniki, pp. 409–421.

Rowe, G.M., 1993. *Performance of asphalt mixtures in the trapezoidal fatigue test*. Proceedings of the Association of Asphalt Paving Technologists, Vol. 62, pp. 344–384.

Rowe, G.M. and Bouldin, M.G., 2000. *Improved techniques to evaluate the fatigue resistance of asphaltic mixtures*. Proceedings of the 2nd Eurasphalt & Eurobitume Congress, Barcelona, Vol. 1, pp. 754–763.

Tayebali, A.A., Deacon, J.A., Coplantz, J.S., Harvey, J.T. and Monismith, C.L., 1992. *Fatigue response of asphalt aggregate-mixes, Part 1 – Test method selection*. Strategic Highway Research Program, SHRP Project A-003A, National Research Council, Washington, D.C.

Thom, N.H., Choi, Y.K. and Harireche, O., 2002. *The influence of aggregate properties on asphalt performance*. Proceedings of the 3rd International Conference Bituminous Mixtures and Pavements, Thessaloniki, pp. 593–602.